

Electronic properties of small model compounds that undergo excited-state intramolecular proton transfer as measured by electroabsorption spectroscopy

Lavanya L. Premvardhan¹, Linda A. Peteanu*

Department of Chemistry, Carnegie Mellon University, Pittsburgh, PA 15213, USA

Received 10 May 2002; received in revised form 27 June 2002; accepted 28 June 2002

Abstract

Electroabsorption (Stark spectroscopy) is used to measure the electronic properties of *o*-hydroxybenzaldehyde (*o*HBA) and *o*-hydroxyacetophenone (*o*HAP), two molecules that undergo excited-state intramolecular proton transfer (ESIPT) in a non-interacting organic glass matrix. We report the change in dipole moment, $|\Delta\vec{\mu}|$, and the average change in polarizability, $\overline{\Delta\alpha}$, for both *o*HBA and *o*HAP as well as for a molecular analog of *o*HAP, *o*-methoxyacetophenone (*o*MAP), in which proton transfer is blocked by methyl substitution. The experimental results for the two ESIPT molecules are found to compare well to the results of ab initio calculations. In contrast, the measured values of $|\Delta\vec{\mu}|$ and $\overline{\Delta\alpha}$ for these systems compare poorly to the INDO/SCI results. Preparation for ESIPT in the Franck–Condon region of the potential energy surface in *o*HAP and *o*HBA is apparent from the calculated atomic charge distributions as an increase of the intramolecular hydrogen bond strength and a decrease in the aromaticity of the phenyl ring.

© 2002 Elsevier Science B.V. All rights reserved.

Keywords: Electroabsorption; Stark; Excited-state intramolecular proton transfer; Electronic structure calculations; Ab initio; INDO/SCI

1. Introduction

Excited-state intramolecular proton transfer (ESIPT) has been extensively studied by experimental [1–9] and theoretical methods [6,10–14] as it is a prototypical condensed phase reaction. Information regarding the potential energy surface of molecules that undergo ESIPT is important to further our understanding of the dynamics of this process. The reaction (Scheme 1) occurs via excitation of the ground state ‘normal’ form, N, to N* followed by proton transfer in the excited-state [4,5]. For numerous ESIPT systems studied to date, the initial proton transfer rates are on the order of a few hundred femtoseconds. The tautomer thus formed, T*, emits strongly Stokes-shifted fluorescence, following which a reverse proton transfer occurs from T in the ground state to regenerate N. The four-level nature of ESIPT molecules has made them amenable to a variety of applications. These

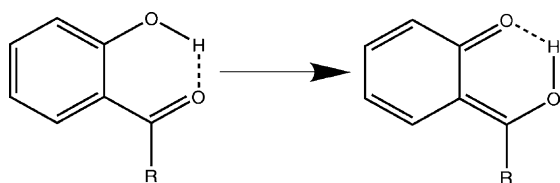
include their use as laser dyes [2,15–17] and as additives to protect polymers from degradation due to exposure to UV light [2,18,19]. Their potential applications in memory storage and optical switching devices has also been explored [2,3].

In electroabsorption spectroscopy, the effect of an external electric field on the absorption spectrum of a sample is measured [20–24]. Analysis of this perturbation yields the magnitude of the change in dipole moment, $|\Delta\vec{\mu}|$, and the average change in polarizability, $\overline{\Delta\alpha}$, between the ground- and excited-states of the absorbing species. These electronic properties for the N → N* transition of molecules that undergo ESIPT are important as they give information about the charge distribution in the excited-state prior to proton transfer. This description of the excited-state potential energy surface in the Franck–Condon region can be used in formulating a mechanism for ESIPT and, in particular, to understand the sensitivity of the process to the properties of the molecular environment. More generally, these quantities are also useful as experimental benchmarks for the accuracy of electronic structure calculations on excited electronic states of reactive species. The importance of accurately modeling the potential energy landscape of ESIPT reactions was highlighted in a recent feature article by Scheiner [10].

Abbreviation: ESIPT, excited-state intramolecular proton transfer; MCH, methyl cyclohexane; *o*HAP, *o*-hydroxyacetophenone; *o*HBA, *o*-hydroxybenzaldehyde; *o*MAP, *o*-methoxyacetophenone; PE, polyethylene

* Corresponding author. Tel.: +1-412-268-1327; fax: +1-412-268-6897.
E-mail address: peteanu@andrew.cmu.edu (L.A. Peteanu).

¹ Present address: Department of Biophysics, Vrije Universiteit, Amsterdam, The Netherlands.



Scheme 1. A general schematic for the ESIPT process in this class of molecules. In *o*HBA, R=H and in *o*HAP, R=CH₃.

We have previously used electroabsorption spectroscopy to determine the electronic properties of several other molecules that undergo ESIPT. For 3-hydroxyflavone (3HF) [25], 2-(2'-hydroxyphenyl)-benzothiazole (HBT) and 2-(2'-hydroxyphenyl)-benzoxazole (HBO) [26] we have found that the dipole moments and polarizabilities of these species do not change drastically upon excitation. In fact, the electroabsorption results for HBT and HBO, verified by solvent-shift analysis and *ab initio* calculations, indicate that the excited-state is actually less polar and less polarizable than the ground state [26]. In the current study we continue this investigation into ESIPT systems by determining the electronic nature of the Franck–Condon region in the N* state of the smallest aromatic molecules that undergo this reaction. The current work focuses on two ESIPT molecules, *o*-hydroxybenzaldehyde (*o*HBA) and *o*-hydroxyacetophenone (*o*HAP), shown in Scheme 1, that have been the subject of numerous theoretical investigations [6,10,12,13,27–39]. We have previously studied *o*HAP in polyethylene (PE) at 298 K [40] and here we extend this investigation to *o*HBA and to *o*-methoxyacetophenone (*o*MAP). *o*MAP is structurally similar to *o*HAP, except that it cannot undergo ESIPT due to the substitution of the intramolecularly bonded hydrogen atom by a methyl group. In this study, the electronic properties of *o*HAP and *o*MAP, the non-proton transfer analogue of *o*HAP, will be compared in order to discern the effects of both an intramolecular hydrogen bond and the presence of the nearby T* state which is expected to be strongly coupled to the initial photo-excited N* state. Electronic structure calculations at the *ab initio* (HF/6-31G*) and semi-empirical (INDO/SCI) levels are presented for comparison to experimental results. In addition, we determine the difference in electronic charge on each atom in the ESIPT molecules between the ground- and excited-states, from *ab initio* calculations, to generate the electronic charge distribution in the Franck–Condon region. Results obtained in polymer matrices will be presented in a future publication.

2. Materials and methods

2.1. Sample preparation

Methyl cyclohexane (MCH), chosen because it is non-polar and does not disrupt the hydrogen bond in *o*HBA and

*o*HAP, was dried by distillation for ≈ 2 h over calcium hydride. A micromolar solution of the probe molecule was prepared with ≈ 5 ml of the distillate. A few microliters of the solution was then injected between the inconel-coated quartz slides that are separated by a kapton spacer. The slides were then clamped together with binder clips and immersed in the liquid nitrogen. Transmission spectra were obtained simultaneously with the Stark spectra so that the same region of the glass is probed for both. The thickness of the sample was determined from the interference patterns in the near IR (900–2000 nm) using an absorption spectrometer (Perkin-Elmer λ_{900}). Interference patterns of the solvent–glass samples were obtained prior to immersing the sample in liquid nitrogen.

2.2. Apparatus

The apparatus and experimental technique for obtaining room-temperature electroabsorption spectra are identical to those described in Ref. [25]. All experiments were performed at a spectral resolution of 5 nm. To obtain electroabsorption spectra at 77 K, a UV-Vis liquid nitrogen immersion dewar (HS Martin) was used.

To change the angle between the externally applied field and the polarization direction of the light from 90° to 54.7° the sample is rotated around an axis perpendicular to the incoming light beam. In order for this angle to be effectively at 54.7°, which is the magic angle (see Section 2.4), the external angle between the sample and the incoming light beam was set at 46° at 77 K to correct for the refractive index change between liquid nitrogen and the MCH glass. In all cases, spectra obtained at the magic angle (54.7°) have been corrected for the refractive index changes mentioned above.

2.3. Electronic structure calculations

Ab initio direct self-consistent field (SCF) calculations were performed using the Gaussian 98 package [41], while semi-empirical INDO/SCI (single-excitation configuration interactions) SCF calculations were performed with the quantum-chemical electronic structure program Argus [42]. Molecular geometries of *o*MAP and the normal, enol forms of *o*HAP and *o*HBA, were optimized using Hartree–Fock (HF) theory and the 6-31G** basis set. The HF/6-31G** optimization yielded geometries for both *o*HBA and *o*HAP in which all the heavy atoms lie in the same plane while, in *o*MAP, the methoxy oxygen is the only heavy atom that lies in the plane of the phenyl ring. The calculated hydrogen bond lengths are 1.883 and 1.799 Å for *o*HBA and *o*HAP, respectively.

Ground state properties were determined from SCF calculations using HF/6-31G* and INDO/SCI. The excited-state was modeled using single-excitation CI in both 6-31G* and INDO/SCI methods. Ground- and excited-state polarizabilities (α) were obtained from finite field (FF) calculations,

Table 1
Comparison of calculated and measured properties of *o*HBA, *o*HAP, and *o*MAP^a

	$ f \cdot \Delta\vec{\mu} $	$f \cdot \Delta\vec{\mu}$		$f \cdot \overline{\Delta\alpha} \cdot f$	$f \cdot \overline{\Delta\alpha} \cdot f$	
	Experimental	6-31G*	INDO/SCI	Experimental	6-31G*	INDO/SCI
<i>o</i> HBA	2.2 ± 0.1	2.04	3.88	4.6 ± 0.6	2.67	9.9
<i>o</i> HAP	2.1 ± 0.1	1.92	3.23	4.4 ± 0.7	2.78	9.4
<i>o</i> MAP	2.6 ± 0.4	1.19	1.25	8.4 ± 1.6	3.54	3.55

^a Dipole moments are in D and polarizabilities in Å³. Gas-phase calculated values of $|\Delta\vec{\mu}|$ and $\overline{\Delta\alpha}$ are scaled by the reaction field in methylcyclohexane glass as well as by the cavity field factor, f , for an ellipsoidal cavity (see text).

in which a field of 0.001 a.u. ($\approx 5 \times 10^6$ V/cm) is applied independently in the x , y and z directions, in order to determine the diagonal elements of the tensor $\underline{\Delta\alpha}$. The values of $\Delta\mu$ represent the vectorial difference of the ground- and excited-state dipole moments, wherein information about both the magnitude and sign of the change in dipole moment is contained. The calculated value of $\Delta\mu$ for all three molecules is positive (Table 1). The change in dipole moment in the direction of the transition moment, $\hat{m} \cdot \Delta\vec{\mu}$, has also been determined and compared to the experimental results.

2.4. Analysis of electroabsorption spectra

The electroabsorption spectrum, corresponding to the change in the absorption spectrum due to the application of an external electric field, according to the formalism of Liptay is fit to the weighted sum of zeroth, first, and second-derivatives of the unperturbed (field-free) absorption spectrum, as proposed by Liptay and co-workers [20–23], and Bublitz and Boxer [24]. The relative contributions of these functions to the overall lineshape are functions of the angle, χ , between the applied AC electric field vector and the electric field vector of the polarized light, and are designated a_χ , b_χ and c_χ , respectively:

$$\begin{aligned} & \frac{2\sqrt{2}}{\ln(10)} \frac{\Delta I}{I} \\ &= \Delta A(\tilde{\nu}) = \vec{F}_{\text{eff}}^2 \left[a_\chi A(\tilde{\nu}) + \frac{b_\chi \tilde{\nu}}{15h} \left\{ \frac{\partial}{\partial \tilde{\nu}} \left(\frac{A(\tilde{\nu})}{\tilde{\nu}} \right) \right\} \right. \\ & \quad \left. + \frac{c_\chi \tilde{\nu}}{30h^2} \left\{ \frac{\partial^2}{\partial \tilde{\nu}^2} \left(\frac{A(\tilde{\nu})}{\tilde{\nu}} \right) \right\} \right] \end{aligned} \quad (1)$$

Experimentally, the change in transmitted light intensity, ΔI , due to the application of an electric field, is measured and normalized by the total light intensity, I , reaching the detector. The absorbance of the sample is expressed in Eq. (1) as $A(\tilde{\nu})$ and is a function of the wavenumber, $\tilde{\nu}$. \vec{F}_{eff} is the effective field at the site of the solute molecule and it includes an enhancement to the applied electric field that is due to the cavity field factor [21]. The coefficients of the derivatives, a_χ , b_χ and c_χ are related to the molecular parameters of interest as shown in the follow-

ing expressions:

$$\begin{aligned} a_\chi &= \frac{1}{30|\vec{m}|^2} \sum_{i,j} [10A_{ij}^2 \\ & \quad + (3A_{ii}A_{jj} + 3A_{ij}A_{ji} - 2A_{ij}^2)(3\cos^2\chi - 1)] \\ & \quad + \frac{1}{15|\vec{m}|^2} \sum_{i,j} [10m_i B_{ij} \\ & \quad + (3m_i B_{jj} + 3m_i B_{ji} - 2m_i B_{ij})(3\cos^2\chi - 1)] \end{aligned} \quad (2)$$

$$\begin{aligned} b_\chi &= \frac{1}{|\vec{m}|^2} \sum_{i,j} [10m_i A_{ij} \Delta\mu_j + (3m_i A_{ji} \Delta\mu_j \\ & \quad + 3m_i A_{jj} \Delta\mu_i - 2m_i A_{ij} \Delta\mu_j)(3\cos^2\chi - 1)] \\ & \quad + \frac{15}{2} \overline{\Delta\alpha} + \frac{3}{2} [\Delta\alpha_m - \overline{\Delta\alpha}](3\cos^2\chi - 1) \end{aligned} \quad (3)$$

$$c_\chi = 5|\overline{\Delta\mu}|^2 + |\overline{\Delta\mu}|^2 [(3\cos^2\xi - 1)(3\cos^2\chi - 1)] \quad (4)$$

Here, ξ is the angle between $\overline{\Delta\mu}$ and \vec{m} , the transition moment vector. In Eq. (3), $\Delta\alpha_m$ (which is $\hat{m} \cdot \underline{\Delta\alpha} \cdot \hat{m}$) corresponds to the magnitude of the change in polarizability in the direction of the transition moment. In each case, if the experiment is performed at the magic angle ($\chi = 54.7^\circ$) the expressions are simplified because $(3\cos^2\chi - 1)$ is equal to zero. These equations are pertinent to the case where the molecules are in a frozen isotropic orientation, as is the case in the studies presented here.

In this work we quote $\overline{\Delta\alpha}$ which represents the average change in electronic polarizability between the ground- and excited-state (i.e. $\overline{\Delta\alpha} = \frac{1}{3}\text{Tr}(\underline{\Delta\alpha})$). The tensors \underline{A} and \underline{B} represent the transition polarizability and hyper-polarizability, respectively. These describe the effect of \vec{F}_{eff} on the molecular transition moment:

$$\vec{m}(\vec{F}_{\text{eff}}) = \vec{m} + \underline{A}\vec{F}_{\text{eff}} + \vec{F}_{\text{eff}}\underline{B}\vec{F}_{\text{eff}}$$

Generally, this term can be neglected for strongly allowed transitions. Moreover, for a small $|\Delta\vec{\mu}|$, such as those measured for the molecules studied here (see Section 3), the cross terms involving the elements of the tensor \underline{A} can be neglected compared to the other terms in the expression for $\overline{\Delta\alpha}$ (Eq. (3)).

Information regarding $|\Delta\vec{\mu}|$ for the molecule is contained in the c_χ term (Eq. (4)). It is important to emphasize that, for an isotropic sample such as those studied in this work, only the magnitude and not the sign of $\Delta\mu$ is measured. For a more detailed discussion of these effects, see Refs. [21,24].

The experiment is normally performed at two angles, $\chi = 54.7^\circ$ (magic angle) and $\chi = 90^\circ$. The utility of measurements at these two angles is that, at $\chi = 54.7^\circ$ and 90° the coefficients c_χ are reduced to:

$$c_{54.7} = 5|\Delta\vec{\mu}|^2 \quad (5)$$

$$c_{90} = 5|\Delta\vec{\mu}|^2 - |\Delta\vec{\mu}|^2(3\cos^2\xi - 1) \quad (6)$$

Similarly, at $\chi = 54.7^\circ$ and 90° , respectively, the coefficients b_χ are reduced to:

$$b_{54.7} = \frac{10}{|\vec{m}|^2} \sum_{i,j} m_i A_{ij} \Delta\mu_j + \frac{15}{2} \overline{\Delta\alpha} \quad (7)$$

$$b_{90} = \frac{3}{|\vec{m}|^2} \sum_{i,j} [4m_i A_{ij} \Delta\mu_j - m_i A_{ji} \Delta\mu_j - m_i A_{ji} \Delta\mu_i] + \frac{15}{2} \overline{\Delta\alpha} + \frac{3}{2} [\overline{\Delta\alpha} - \Delta\alpha_m] \quad (8)$$

As noted earlier, the terms containing the transition moment polarizability tensor, A , can be neglected in the expressions for b_{90} and $b_{54.7}$ (Eqs. (7) and (8)) as they are expected to be small in comparison to the other terms. Hence the expressions for b_{90} and $b_{54.7}$ are reduced to the form:

$$b_{54.7} \approx \frac{15}{2} \overline{\Delta\alpha} \quad (9)$$

$$b_{90} \approx \frac{15}{2} \overline{\Delta\alpha} + \frac{3}{2} [\overline{\Delta\alpha} - \Delta\alpha_m] \quad (10)$$

The change in the static electronic polarizability in the direction of the transition moment is then:

$$\Delta\alpha_m = \frac{12b_{54.7} - 10b_{90}}{15} \quad (11)$$

and the change in dipole moment along the transition moment is:

$$|m \cdot \Delta\vec{\mu}| = \sqrt{\frac{6c_{54.7} - 5c_{90}}{15}} \quad (12)$$

The coefficients, a_χ , b_χ and c_χ , are extracted by means of a linear least-squares fit of the electroabsorption signal to the sum of derivatives of the absorption spectrum, using a program written in MATLAB (Mathworks). The details of the procedure we use to fit the electroabsorption spectrum to the derivatives of the absorption spectrum have been previously described in Ref. [25].

2.5. Comparison of gas-phase calculations to condensed phase measurements

In order to compare the measured and calculated values of $\Delta\mu$ and $\overline{\Delta\alpha}$, the degree of amplification of the

applied electric field by the medium must be accounted for with the appropriate cavity field [20–22]. In addition, the enhancement of $\Delta\mu$ and $\overline{\Delta\alpha}$ that arises due to polarization of the medium, or the reaction field, must also be included. The values of $\Delta\mu$ and $\overline{\Delta\alpha}$, obtained from gas-phase calculations, have therefore been scaled by reaction and cavity field factors [21] in order to permit a direct comparison with condensed phase experimental results. To apply these corrections, it is necessary to accurately model the cavity in which the molecule resides. The cavity and reaction field corrections for a spherical cavity formulated by Onsager [43] were modified for an ellipsoid, so as to better mimic the actual shape of the molecules studied here [44]. The molecular cavities used have the following dimensions for the semi-axes of the ellipsoid: $a_x = 4.05 \text{ \AA}$, $a_y = 3.95 \text{ \AA}$, and $a_z = 1.2 \text{ \AA}$ for *o*HBA, $a_x = 4.57 \text{ \AA}$, $a_y = 4.03 \text{ \AA}$, and $a_z = 2.08 \text{ \AA}$ for *o*HAP and $a_x = 4.85 \text{ \AA}$, $a_y = 4.33 \text{ \AA}$, and $a_z = 2.6 \text{ \AA}$ for *o*MAP. The lengths of the semi-axes are the actual molecular dimensions as obtained from HF/6-31G** optimized structures, augmented by 1.2 \AA , estimated as the van der Waals radius of hydrogen [45].

A detailed explanation of the determination of the shape factors and its application in determining the cavity field is reported in Ref. [26]. As the dipole moment of the molecules lie in the *XY* plane, we have multiplied the *x* and *y* components of calculated gas-phase values of $\Delta\mu$ by the field factors in the *x* and *y* directions, f_x and f_y , respectively, while the gas-phase values of $\overline{\Delta\alpha}$ were multiplied by the average of the sum of squares of f_x and f_y . We have applied reaction field corrections in a similar manner. The dielectric constants and refractive indices that have been used for this scaling have been reported in Ref. [46]. The room-temperature parameters of the static dielectric constant, ϵ_0 , and refractive index, *n*, for MCH have also been used at low-temperatures as it is relatively non-polar.

3. Results

3.1. Electroabsorption data

The electroabsorption spectra of *o*HBA, *o*HAP and *o*MAP in MCH at 77 K obtained with χ set at 54.7° and at 90° are shown in Figs. 1–3. In all cases, the electroabsorption spectra have been fit to derivatives of the experimental absorption spectra (Eq. (1)). Deviations between the electroabsorption spectra (solid lines) and these fits (dashed lines) indicate that the field response is not uniform across the absorption band [24,47]. In such cases, the electroabsorption signal is presumably a composite of the field response arising from more than one electronic transition or from conformers of the molecule having differing electronic properties. Small deviations of this type occur for all three molecules, primarily to the high-energy side of the spectra where there may be interference with the higher-lying absorption transition. The

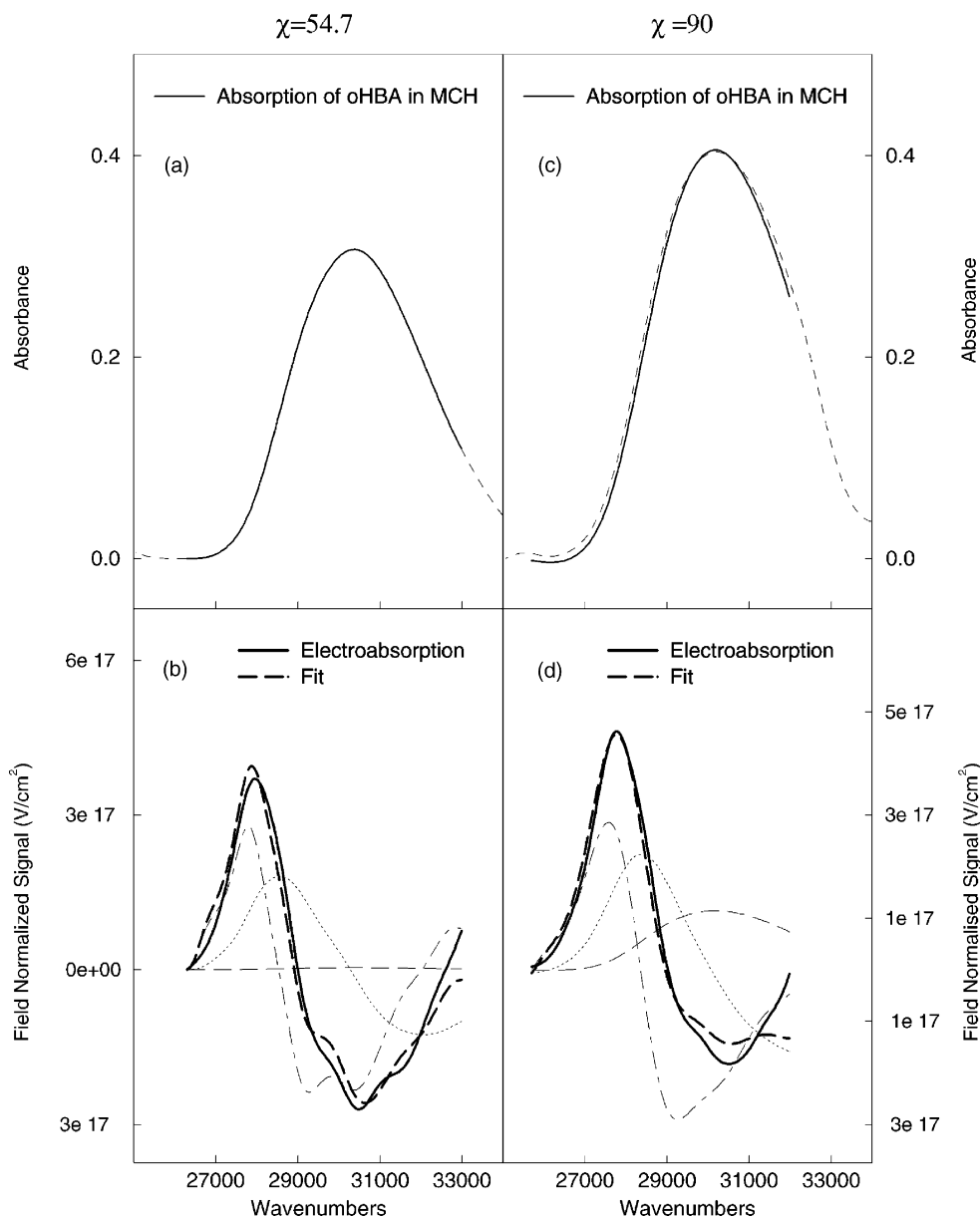


Fig. 1. (a) Absorption of *o*HBA in MCH glass. The dashed line shows the entire absorption spectrum and the solid line denotes the region used for the fit to the electroabsorption spectrum. (b) Electroabsorption (bold solid line) and fit (bold dashed line) of *o*HBA in MCH glass at $\chi = 54.7^\circ$. Also shown are the individual components of the fit, which are the zeroth (dash), first (dot) and second (dash-dot) derivatives of the absorption spectrum. Panels (c) and (d) contain the analogous data obtained at $\chi = 90^\circ$.

lineshapes of the electroabsorption signals will be discussed below in greater detail.

Our determinations of the molecular parameters, $\overline{\Delta\alpha}$ and $|\Delta\vec{\mu}|$ are listed in Table 1. In all cases, the reported $\overline{\Delta\alpha}$'s are those obtained directly from the fitting coefficient $b_{54.7}$ (Eq. (3)). Each value reported represents the average of between 3 and 5 independent experimental determinations.

Table 1 also contains the corresponding values of $\Delta\mu$ and $\overline{\Delta\alpha}$ calculated from both ab initio (HF/6-31G*) and semi-empirical (INDO/SCI) methods. The gas-phase values have been scaled by the cavity and reaction fields that would be experienced by the probe molecule in the solvent-glass

environment. Overall, there is reasonable agreement between the experimental values of $|\Delta\vec{\mu}|$ and ab initio calculations for all three molecules. However, in the case of *o*HBA and *o*HAP, results from INDO/SCI calculations are a factor of two larger than experiment. In contrast, agreement between ab initio and INDO/SCI calculations is quite good for the non-proton transfer molecule, *o*MAP, though both results are somewhat smaller than the experimental values.

The fits to the electroabsorption spectra obtained with the angle between the electric field vector of the light beam and the applied electric field, χ , set at 90° , yield values for the change in static electronic polarizability in the direction

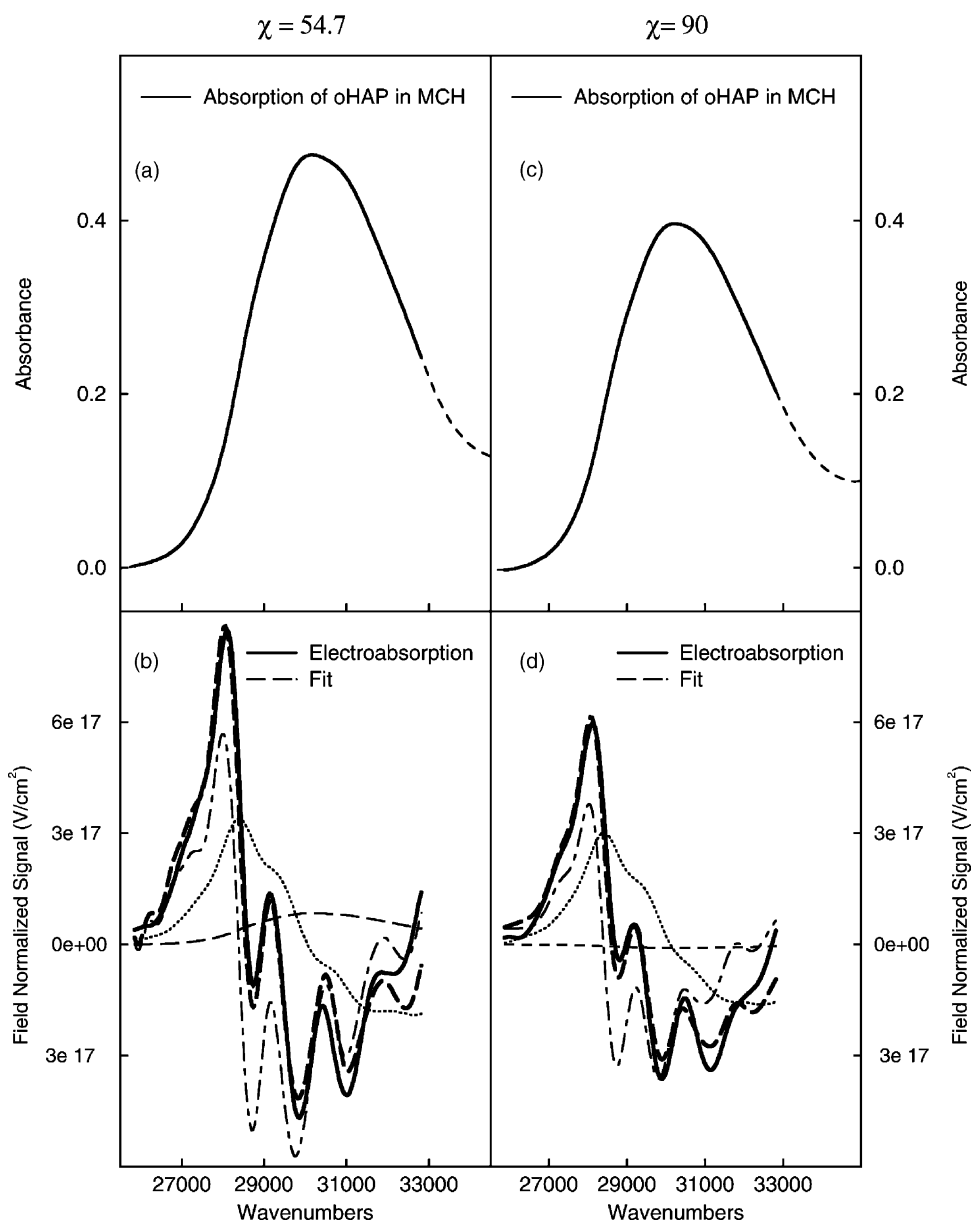


Fig. 2. (a) Absorption of *o*HAP in MCH glass. The dashed line shows the entire absorption spectrum and the solid line denotes the region used for the fit to the electroabsorption spectrum. (b) Electroabsorption (bold solid line) and fit (bold dashed line) of *o*HAP in MCH glass at $\chi = 54.7^\circ$. Also shown are the individual components of the fit, which are the zeroth (dash), first (dot) and second (dash-dot) derivatives of the absorption spectrum. Panels (c) and (d) contain the analogous data obtained at $\chi = 90^\circ$.

of the transition moment, $\Delta\alpha_m$, and the angle between the change in dipole moment and the transition moment, $|\hat{m} \cdot \Delta\vec{\mu}|$ (Eqs. (11) and (12)). The corresponding data and fits are shown in Figs. 1–3 and the values are reported in Table 2.

In order to obtain additional information about the anisotropy in the change in electronic charge distribution on excitation, the average change in electronic polarizability, $\overline{\Delta\alpha}$ (Table 1) may be compared to $\Delta\alpha_m$ (Table 2). We find that $\Delta\alpha_m$ is equal to $3\overline{\Delta\alpha}$ for *o*MAP, indicating that the major component of the change in polarizability occurs in the direction of the transition moment. In contrast, for *o*HAP and *o*HBA, $\Delta\alpha_m$ is significantly less than $3\overline{\Delta\alpha}$, in-

Table 2
Experimental and calculated properties in MCH glass^a

	$ \hat{m} \cdot \Delta\vec{\mu} (\theta)$		$\Delta\alpha_m$
	6-31G*	Experimental	Experimental
<i>o</i> HBA	1.576 (18°)	1.8 ± 0.4 (35)	7 ± 4
<i>o</i> HAP	1.657 (18°)	1.8 ± 0.2 (31)	6.0 ± 2
<i>o</i> MAP	0.576 (24°)	2.4 ± 0.5 (20)	22 ± 5

^a Values of $|\hat{m} \cdot \Delta\vec{\mu}|$ are reported in D and $\Delta\alpha_m(\hat{m} \cdot \Delta\alpha \cdot \hat{m})$ in \AA^3 . The angle between the transition moment and difference dipole moment (θ) is reported in parentheses. The experimental value of θ reported here is obtained from the mean value $|\hat{m} \cdot \Delta\vec{\mu}|$ and $|\Delta\vec{\mu}|$, where \hat{m} corresponds to a unit vector in the direction of the transition moment.

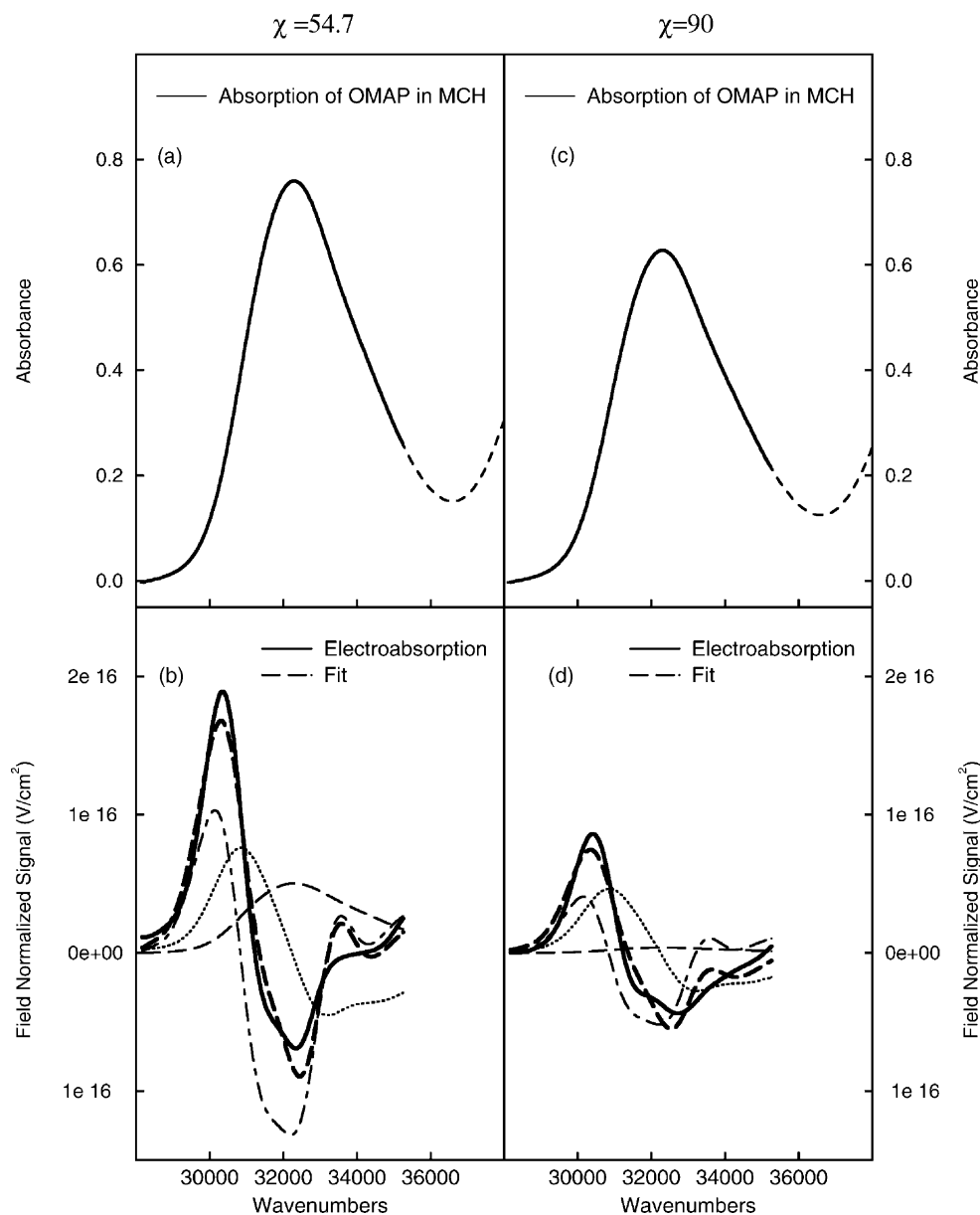


Fig. 3. (a) Absorption of *o*MAP in MCH glass. The dashed line shows the entire absorption spectrum and the solid line denotes the region used for the fit to the electroabsorption spectrum. (b) Electroabsorption (bold solid line) and fit (bold dashed line) of *o*MAP in MCH glass at $\chi = 54.7^\circ$. Also shown are the individual components of the fit, which are the zeroth (dash), first (dot) and second (dash-dot) derivatives of the absorption spectrum. Panels (c) and (d) contain the analogous data obtained at $\chi = 90^\circ$.

dicating that the change in polarizability on excitation is not primarily along the direction of the transition moment. Nonetheless, it is likely to lie in the molecular plane as *ab initio* calculations indicate that $\Delta\alpha_{zz}$, which is the component of $\Delta\alpha$ in the direction perpendicular to the plane of the molecule, is negligible.

3.2. *Ab initio* Mulliken charge analysis of the optical transition

The *ab initio* method was used to determine the change in atomic charge between the excited and ground state

for each atom in all three molecules because it better describes the properties of the N^* state in the ESIPT molecules than does INDO/SCI judging by comparison to our experimental results. The change in charge distribution on each atom allows us to determine two quantities relevant to the ESIPT mechanism (see Scheme 1). The first is the relative extent of electron de-localization on each atom. This provides a measure of the aromaticity present in the phenyl rings. The second is that it identifies the region of the molecule in which the charge redistribution that accompanies the $N \rightarrow N^*$ excitation is localized.

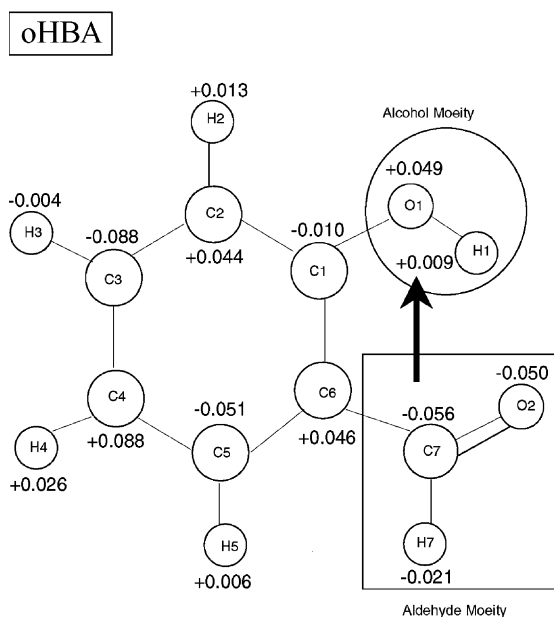


Fig. 4. Pictorial representation of the changes in the partial charges on each of the atoms of *o*HBA following optical excitation ($N \rightarrow N^*$). The circle highlights the proton-donor region of the molecule and the rectangle highlights the proton-acceptor region. The bold arrow represents the direction of the net change in dipole moment on excitation.

An examination of the ground state charge distribution (data not shown) indicates that, in all three molecules, the electronic charge is not equally distributed over C1 through C6 due to the presence of electron-withdrawing or donat-

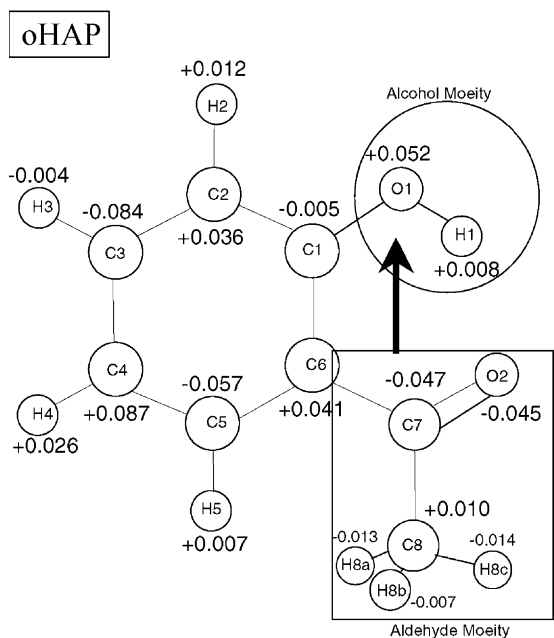


Fig. 5. Pictorial representation of the changes in the partial charges on each of the atoms of *o*HAP following optical excitation ($N \rightarrow N^*$). The circle highlights the proton-donor region of the molecule and the rectangle highlights the proton-acceptor region. The bold arrow represents the direction of the net change in dipole moment on excitation.

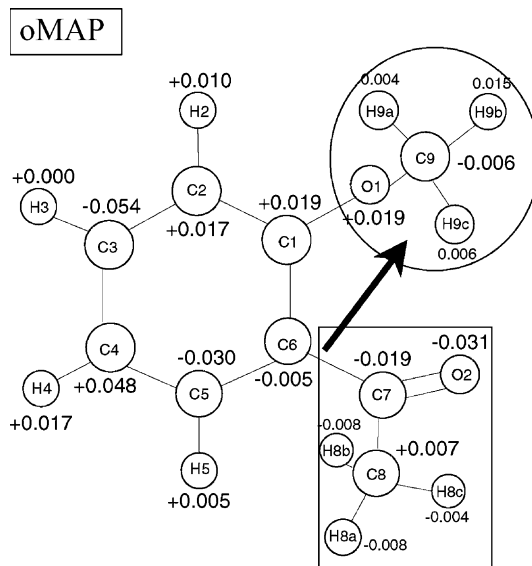


Fig. 6. Pictorial representation of the changes in the partial charges on each of the atoms of *o*MAP following optical excitation. The circle highlights the methoxy region of the molecule and the rectangle highlights the aldehyde region. The bold arrow represents the direction of the net change in dipole moment on excitation.

ing substituents that tend to decrease the aromaticity of the phenyl ring. However, on excitation, the amount of charge on the phenyl carbon atoms C2–C5 in *o*HBA and *o*HAP alternately increases and decreases by roughly a factor of two more than does the charge on the corresponding atoms of *o*MAP (see Figs. 4–6). This alternating increase and decrease in electronegativity of C1–C6 in the ES IPT molecules is indicative of a loss in aromaticity in these systems that is greater than that evident in *o*MAP. This effect and its implications for the ES IPT process will be discussed in greater detail below.

Considering changes in electron density in the region of the molecule where ES IPT occurs, atoms C7 and O2 in the aldehyde proton-acceptor moiety of *o*HAP and *o*HBA exhibit an increase in electron density in the excited-state that is a factor of ~ 2 greater than that seen in the corresponding atoms of *o*MAP (Figs. 4–6). Concomitantly, the donor atom O1 becomes somewhat more electropositive in the ES IPT molecules than in *o*MAP. These changes in electron density would be expected to favor proton transfer from O1 to O2. It is interesting to note that the favorability for proton transfer is already reflected in the degree of charge separation in the Franck–Condon region of the N^* state in the ES IPT molecules.

4. Discussion

Here, we will discuss the results from experimental measurements and electronic structure calculations of the electronic properties of *o*HBA, *o*HAP and *o*MAP.

Both *o*MAP and the proton transfer molecules, *o*HBA and *o*HAP exhibit a moderate increase in polarity on excitation that is reflected in the values for $|\Delta\bar{\mu}|$ of ≈ 1.5 – 2 D. Because ESIPT is mediated primarily by a strengthening of the intramolecular hydrogen bond [3,5,10], most of the change in charge distribution that occurs on excitation would be expected to be confined to this small region of the molecule. This is consistent with the results of calculations. In fact, Figs. 4 and 5 show that the change in dipole moment occurs primarily due to charge separation between the aldehyde moiety (C7-O2-H7 in *o*HBA and C7-O2-C8H3 in *o*HAP) and the OH group moiety in the ESIPT molecules. Therefore, charge separation over 1.5 – 2 Å on the order of 0.15 – 0.20 e^- that occurs between the alcohol and aldehyde moieties, is consistent with the change in dipole moment on the order of 1 – 2 D that is measured experimentally. In the non-ESIPT molecule *o*MAP, the direction of the overall change in dipole moment points instead between the phenyl ring and the methoxy group (Fig. 6).

In molecules that undergo ESIPT, the strengthening of the intramolecular hydrogen bond that occurs in the excited-state is accompanied by a loss in aromaticity in the phenyl ring (Scheme 1). If the extent of aromaticity can indeed be correlated to the value of $\overline{\Delta\alpha}$, then there is some evidence for this effect in that the change in polarizability of *o*HAP is somewhat smaller than that of its non-proton transfer analogue *o*MAP (Table 1). Therefore, the decrease in aromaticity that is predicted to result from proton transfer (Scheme 1) may also be manifested to some degree in the Franck–Condon region. This hypothesis is suggested by the atomic charge distribution analysis (see Section 3). However, we note that the value of $\overline{\Delta\alpha}$ predicted by ab initio calculations is not significantly larger for *o*MAP as compared to *o*HAP. The somewhat greater difference in the experimental values of $\overline{\Delta\alpha}$ may therefore, be an indication that there is actually a comparatively greater degree of electron localization in the ESIPT systems in the condensed phase than is predicted from the calculated gas-phase charge distribution analysis.

4.1. Lineshape of the electroabsorption signal

An interesting feature of the electroabsorption signal of *o*HAP in the low-temperature MCH matrix is the presence of obvious vibronic progression in which the peaks are separated by ≈ 1100 cm^{-1} (Fig. 2). This mode corresponds to the 1326 cm^{-1} stretch of the substituted benzene ring seen in the resonance Raman spectrum [9]. The substantial drop in frequency of this mode in the excited-state relative to the ground state is indicative that there is a significant decrease in the stiffness of the bonds associated with the ring stretching mode. The fact that the fit to this highly structured electroabsorption lineshape is quite good indicates that the electronic properties are quite similar for the different vibronic states in N^* . In contrast, we have previously found that there is evidence for variation in the electronic

properties between various vibronic levels in the absorption manifold in HBT and HBO [26]. Such resolution of the absorption band is not present in either *o*HBA or *o*MAP at 77 K. This may reflect a higher degree of mixing of the $n-\pi^*$ and $\pi-\pi^*$ states in these other molecules versus *o*HAP. Likewise, if multiple conformers of these molecules are present, this may also diminish the spectral resolution.

Comparing the electroabsorption lineshape of *o*HAP in MCH glass to that previously published using room-temperature PE as a matrix, we find that the temperature and properties of the matrix has a noticeable effect on the appearance of the electroabsorption spectrum. Specifically, the electroabsorption spectrum in room-temperature PE (Fig. 2 of Ref. [40]) contained a substantial contribution from the zeroth derivative (a_χ , Eq. (2)) of the absorption spectrum when compared to that in MCH glass. Likewise, the contribution of the first derivative (b_χ , Eq. (3)) is larger in the spectrum taken from the PE sample than that shown here. We have previously shown [46,48] that the electroabsorption spectra of molecules in flexible matrices that are above their glass-transition temperature, such as PE at 298 K, will exhibit enhanced first- and second-derivative contributions that arise due to re-orientation of the molecule in the applied field. Such re-orientation is eliminated in MCH at 77 K. A preliminary model for this effect was published in Refs. [46,48] and a more detailed examination is in progress. While in Refs. [46,48] we found dramatic effects on the electronic properties derived from electroabsorption due to re-orientation, this did not turn out to be the case in *o*HAP [40].

4.2. Comparison to calculations

We have used both ab initio and semi-empirical methods to determine the electronic properties of all three probes and compared them to the experimentally determined properties. Overall, we find good agreement between experiment and ab initio results for the ESIPT molecules. As in previous studies, we find that INDO/SCI calculations do not accurately describe the electronic properties of the reactive excited-state that undergoes proton transfer [25,26]. This may be seen in the fact that both $\Delta\mu$ and $\overline{\Delta\alpha}$ calculated using INDO/SCI are consistently larger than ab initio results, though the corresponding ground state properties are similar (data not shown). We have likewise found that INDO calculations on other ESIPT molecules such as 3HF show good agreement with experiment only for those higher-lying electronic states in which proton transfer does not occur. We therefore, conjecture that the INDO methodology is unable to accurately calculate the properties of the N^* state due to the empirical parameterization used in the calculation procedure.

It is interesting to note that INDO/SCI and ab initio methods predict similar properties for the non-proton transfer molecule, *o*MAP. This too demonstrates that, for non-ESIPT systems, the two methods are in good agreement. However,

the agreement between the calculated and measured properties of *o*MAP in methylcyclohexane glass is not as good as was seen for the ESIPT molecules. We hypothesize that the discrepancy arises due to the presence of multiple conformers of *o*MAP in the sample and/or the possibility that the conformer that is favored in the gas-phase optimization is not that found in the glass. Calculations of $\Delta\mu$ as a function of twist angle of the methyl group (C9(H9)₃ in Fig. 6) show that its value increases by $\sim 20\%$ as the twist angle increases from 37.4° (optimized value) to 110° bringing experiment and calculation into better agreement. It is likely that the geometry of *o*MAP would be more sensitive to environmental perturbations than that of the ESIPT molecules because, in the latter, the favored geometry is stabilized by the formation of a strong intramolecular hydrogen bond.

5. Conclusions

The proton transfer molecules studied here exhibit small values for the change in polarizability ($< 10 \text{ \AA}^3$) and in dipole moment ($\approx 1\text{--}2 \text{ D}$) on excitation that are predicted accurately by ab initio calculations. Using ab initio methods the overall change in atomic charge distribution was found to be confined to the proton-donor and proton-acceptor groups. Furthermore, the weakening of the intramolecular hydrogen bond and decrease in aromaticity that are characteristic of the ESIPT process were discerned from the computational results.

Acknowledgements

We would like to acknowledge our sources of funding, the NSF CAREER and NSF 0109761 programs and the Center for Molecular Analysis at CMU for the use of the absorption spectrometer. LLP would like to thank Sudha Dorairaj and Prof. Robert Stewart and Prof. Hyung J. Kim for the useful discussions and insightful suggestions.

References

- [1] P.K. Sengupta, M. Kasha, Excited state proton-transfer spectroscopy of 3-hydroxyflavone and quercetin, *Chem. Phys. Lett.* 68 (1979) 382–385.
- [2] A.U. Acuna, F. Amat-Guerri, A. Costela, A. Douhal, J.M. Figuera, F. Florido, R. Sastre, Proton-transfer lasing from solid organic matrices, *Chem. Phys. Lett.* 187 (1991) 98–102.
- [3] T. Nishiyama, S. Yamauchi, N. Hirota, M. Baba, I. Hanazaki, Fluorescence studies of the intramolecularly hydrogen-bonded molecules *o*-hydroxyacetophenone and salicylamide and related molecules, *J. Phys. Chem.* 90 (1986) 5730–5735.
- [4] B.A. Schwartz, L.A. Peteanu, C.A. Harris, Direct observation of fast proton transfer: femtosecond photophysics of 3-hydroxyflavone, *J. Phys. Chem.* 96 (1992) 3591–3598.
- [5] P.F. Barbara, P.K. Walsh, L.E. Brus, Picosecond kinetic and vibrationally resolved spectroscopic studies of intramolecular excited-state hydrogen atom transfer, *J. Phys. Chem.* 93 (1989) 29–34.
- [6] J. Catalàn, J.C.D. Valle, C. Diaz, J. Palomar, J.L.G. de Paz, M. Kasha, Solvatochromism of fluorophores with an intramolecular hydrogen bond and their use as probes in biomolecular cavity sites, *Int. J. Quantum Chem.* 72 (1999) 421–438.
- [7] C. Chudoba, E. Riedle, M. Pfeiffer, T. Elsaesser, Vibrational coherence in ultrafast excited state proton transfer, *Chem. Phys. Lett.* 263 (1996) 622–628.
- [8] K. Tokumura, O. Oyama, H. Mukaihata, M. Itoh, Rotational isomerization of phototautomer produced in the excited-state proton transfer of 2,2'-bipyridin-3-ol, *J. Phys. Chem. A* 101 (1997) 1419–1421.
- [9] L.A. Peteanu, R.A. Mathies, Resonance Raman intensity analysis of the excited-state proton transfer in 2-hydroxyacetophenone, *J. Phys. Chem.* 96 (1992) 6910–6916.
- [10] S. Scheiner, Theoretical studies of excited-state proton transfers in small model systems, *J. Phys. Chem. A* 104 (2000) 5898–5909.
- [11] S.-I. Nagaoka, U. Nagashima, Intramolecular proton transfer in various electronic states of *o*-hydroxybenzaldehyde, *Chem. Phys.* 136 (1989) 153–163.
- [12] J.J. i Timoneda, J.T. Hynes, Nonequilibrium free energy surfaces for hydrogen-bonded proton-transfer complexes in solution, *J. Phys. Chem.* 95 (1991) 10431–10442.
- [13] J. Catalàn, C. Diaz, Induction of triplet-state emission of the transient proton-transfer keto form of methyl salicylate by heavy-atom perturbation, *J. Phys. Chem. A* 102 (1998) 323.
- [14] J. Catalàn, J. Palomar, J.L.G. de Paz, Intramolecular proton or hydrogen-atom transfer in the ground and excited states of 2-hydroxybenzoyl compounds, *J. Phys. Chem. A* 101 (1997) 7914–7921.
- [15] P. Chou, D. McMorro, T.J. Aartsma, M. Kasha, The proton-transfer laser. Gain spectrum and amplification of spontaneous emission of 3-hydroxyflavone, *J. Phys. Chem.* 88 (1984) 4596–4599.
- [16] P. Chou, T.J. Aartsma, The proton-transfer laser. Dual wavelength lasing action in binary dye mixtures involving 3-hydroxyflavone, *J. Phys. Chem.* 90 (1986) 721–723.
- [17] D.A. Parthenopoulos, D. McMorro, M. Kasha, Comparative study of stimulated proton-transfer luminescence of three chromones, *J. Phys. Chem.* 95 (1991) 2668–2674.
- [18] H.J. Heller, H.R. Blattmann, Stabilization of polymers against light, *Pure Appl. Chem.* 36 (1973) 141–161.
- [19] R.M. Tarkka, S.A. Jenekhe, Effects of electronic delocalization on intramolecular proton transfer, *Chem. Phys. Lett.* 260 (1996) 533–538.
- [20] W. Liptay, Dipole moments of molecules in excited states and the effect of external electric fields on the optical absorption of molecules in solution, in: O. Sinanoglu (Ed.), *Modern Quantum Chemistry: Part III. Action of Light and Organic Crystals*, Academic Press, New York, 1965, pp. 45–66.
- [21] W. Liptay, Dipole moments and polarizabilities of molecules in excited electronic states, in: E.C. Lim (Ed.), *Excited States*, Academic Press, New York, 1974, pp. 129–229.
- [22] W. Liptay, Electrochromism and solvatochromism, *Angew. Chem. Internat. Edit.* 8 (1969) 177–188.
- [23] R. Wortmann, K. Elich, W. Liptay, Excited state dipole moments and polarizabilities of centrosymmetric and dimeric molecules. III. Model calculations for 1,8-diphenyl-1,2,3,7-octatetraene, *Chem. Phys.* 124 (1988) 395–409.
- [24] G.U. Bublitz, S.G. Boxer, Stark spectroscopy: applications in chemistry, biology, and materials science, *Ann. Rev. Phys. Chem.* 48 (1997) 213–242.
- [25] L.L. Premvardhan, L.A. Peteanu, Dipolar properties of and temperature effects on the electronic states of 3-hydroxyflavone (3HF) determined using Stark-effect spectroscopy and compared to electronic structure calculations, *J. Phys. Chem. A* 103 (1999) 7506–7514.
- [26] L. Premvardhan, L. Peteanu, Electroabsorption measurements and ab initio calculations of the dipolar properties of 2-(2'-hydroxyphenyl)benzothiazole and -benzoxazole: two photostabilizers that undergo excited-state proton transfer, *Chem. Phys. Lett.* 296 (1998) 521–529.

- [27] G. Chung, O. Kwon, Y. Kwon, Theoretical study on salicylaldehyde and 2-mercaptobenzaldehyde: intramolecular hydrogen bonding, *J. Phys. Chem. A* 102 (1998) 2381–2387.
- [28] P. George, C.W. Bock, M. Trachtman, Hydrogen bonding in salicylaldehyde: a molecular orbital study, *J. Mol. Struct. (Theochem)* 133 (1985) 11–24.
- [29] H. Lampert, W. Mikenda, A. Karpfen, Intramolecular hydrogen bonding in 2-hydroxybenzoyl compounds: infrared spectra and quantum chemical calculations, *J. Phys. Chem.* 100 (1996) 7418–7425.
- [30] M. Cuma, S. Scheiner, T. Kar, Effect of adjoining aromatic ring upon excited-state proton transfer, *o*-hydroxybenzaldehyde, *J. Mol. Struct.* 467 (1999) 37–49.
- [31] J. Palomar, J.L.G. de Paz, J. Catalàn, Vibrational study of intramolecular hydrogen bonding in *o*-hydroxybenzoyl compounds, *Chem. Phys.* 246 (1999) 167–208.
- [32] L. Rodriguez-Santiago, M. Sodupe, A. Oliva, J. Bertran, Hydrogen atom or proton transfer in neutral and single positive ions of salicylic acid and related compounds, *J. Am. Chem. Soc.* 121 (1999) 8880–8890.
- [33] A.L. Sobolewski, W. Domcke, Theoretical investigation of potential energy surfaces relevant for excited-state hydrogen transfer in *o*-hydroxybenzaldehyde, *Chem. Phys.* 184 (1994) 115–124.
- [34] K.B. Borisenko, C.W. Bock, I. Hargittai, Molecular geometry of benzaldehyde and salicylaldehyde: a gas-phase electron diffraction and ab initio molecular orbital investigation, *J. Phys. Chem.* 100 (1996) 7426–7434.
- [35] V. Barone, C. Adamo, Proton transfer in the ground and lowest excited states of malonaldehyde: a comparative density functional and post-Hartree–Fock study, *J. Chem. Phys.* 105 (1996) 11007–11019.
- [36] J. Catalàn, J. Palomar, J.L.G. de Paz, Intramolecular proton or hydrogen-atom transfer in the ground and excited states of 2-hydroxybenzoyl compounds, *J. Phys. Chem. A* 101 (1997) 7914–7921.
- [37] R.I. Cukier, J. Zhu, Simulation of proton transfer reaction rates: the role of solvent electronic polarization, *J. Phys. Chem. B* 101 (1997) 7180–7190.
- [38] M. Cuma, S. Scheiner, T. Kar, Competition between rotamerization and proton transfer in *o*-hydroxybenzaldehyde, *J. Am. Chem. Soc.* 120 (1998) 10497–10503.
- [39] M.V. Vener, S. Scheiner, Hydrogen bonding and proton transfer in the ground and lowest excited singlet states of *o*-hydroxyacetophenone, *J. Phys. Chem.* 99 (1995) 642–649.
- [40] L. Peteanu, S. Locknar, Stark spectroscopy of an excited-state proton-transfer molecule: comparison of experimental and computational results for *o*-hydroxyacetophenone, *Chem. Phys. Lett.* 274 (1997) 79–84.
- [41] J. Frisch, G.W. Trucks, H.B. Schlegel, G.E. Scuseria, M.A. Robb, J.R. Cheeseman, V.G. Zakrzewski, J.A. Montgomery Jr., R.E. Stratmann, J.C. Burant, S. Dapprich, J.M. Millam, A.D. Daniels, K.N. Kudin, M.C. Strain, O. Farkas, J. Tomasi, V. Barone, M. Cossi, R. Cammi, B. Mennucci, C. Pomelli, C. Adamo, S. Clifford, J. Ochterski, G.A. Petersso, P.Y. Ayala, Q. Cui, K. Morokuma, D.K. Malick, A.D. Rabuck, K. Raghavachari, J.B. Foresman, J. Cioslowski, J.V. Ortiz, B.B. Stefanov, G. Liu, A. Liashenko, P. Piskorz, I. Komaromi, R. Gomperts, R.L. Martin, D.J. Fox, T. Keith, M.A. Al-Laham, C.Y. Peng, A. Nanayakkara, C. Gonzalez, M. Challacombe, P.M.W. Gill, B. Johnson, W. Chen, M.W. Wong, J.L. Andres, C. Gonzalez, M. Head-Gordon, E.S. Replogle, J.A. Pople, Gaussian 98, Revision A.6, Gaussian, Inc., Pittsburgh, 1998.
- [42] M.A. Thompson, Argus (TM), Version 1.2, 1992.
- [43] L. Onsager, Electric moments of molecules in liquids, *J. Am. Chem. Soc.* 58 (1936) 1486–1493.
- [44] C.J.F. Bottcher, Theory of Electric Polarisation, Elsevier, Amsterdam, 1952, p. 492.
- [45] J. Tomasi, M. Persico, Molecular interactions in solution: an overview based on continuous distributions of the solvent, *Chem. Rev.* 94 (1994) 2027–2094.
- [46] A. Chowdhury, S.A. Locknar, L.L. Premvardhan, L.A. Peteanu, Effects of matrix temperature and rigidity on the electronic properties of solvatochromic molecules: an electroabsorption study of Coumarin 153, *J. Phys. Chem. A* 103 (1999) 9614–9625.
- [47] R. Wortmann, K. Elich, W. Liptay, Excited state dipole moments and polarizabilities of centrosymmetric and dimeric molecules. II. Polyenes, polyynes, and cumulenes, *Chem. Phys.* 120 (1988) 439–448.
- [48] S.A. Locknar, A. Chowdhury, L.A. Peteanu, Matrix and temperature effects on the electronic properties of conjugated molecules: an electroabsorption study of all-*trans*-retinal, *J. Phys. Chem. B* 104 (1999) 5816–5824.